J Neurophysiol 91: 2422–2428, 2004.
First published January 28, 2004; 10.1152/jn.01130.2003.

Large Releasable Pool of Synaptic Vesicles in Chick Cochlear Hair Cells

Marc D. Eisen,[2] Maria Spassova,[1] and Thomas D. Parsons[1,2]
[1]*Department of Clinical Studies, New Bolton Center, School of Veterinary Medicine, Kennett Square, 19348; and* [2]*Department of Otorhinolaryngology, Head and Neck Surgery, School of Medicine, University of Pennsylvania, Philadelphia, Pennsylvania 19104*

Submitted 24 November 2003; accepted in final form 13 January 2004

Eisen, Marc D., Maria Spassova, and Thomas D. Parsons. Large releasable pool of synaptic vesicles in chick cochlear hair cells. *J Neurophysiol* 91: 2422–2428, 2004. First published January 28, 2004; 10.1152/jn.01130.2003. Hearing requires the hair cell synapse to maintain notable temporal fidelity (≤1 ms) while sustaining neurotransmitter release for prolonged periods of time (minutes). Here we probed the properties and possible anatomical substrate of prolonged neurotransmitter release by using electrical measures of cell surface area as a proxy for neurotransmitter release to study hair cell exocytosis evoked by repetitive stimuli. We observed marked depression of exocytosis by chick tall hair cells. This exocytic depression cannot be explained by calcium current inactivation, presynaptic autoinhibition by metabotropic glutamate receptors, or postsynaptic receptor desensitization. Rather, cochlear hair cell exocytic depression resulted from the exhaustion of a functional vesicle pool. This releasable vesicle pool is large, totaling approximately 8,000 vesicles, and is nearly 10 times greater than the number of vesicles tethered to synaptic ribbons. Such a large functional pool suggests the recruitment of cytoplasmic vesicles to sustain exocytosis, important for maintaining prolonged, high rates of neural activity needed to encode sound.

INTRODUCTION

Receptor cells in the auditory, vestibular, and visual system encode sensory inputs with graded membrane potentials. These potentials allow for a continuously varying synaptic output. The active zones at these synapses use a specialized structure, the "ribbon" or "dense body" (Lenzi and von Gersdorff 2001; Parsons and Sterling 2003; von Gersdorff 2001), which anchors to the presynaptic membrane only nanometers from the clustered, voltage-gated calcium channels (Issa and Hudspeth 1994; Nachman-Clewner et al. 1999; Roberts et al. 1990). The ribbon tethers synaptic vesicles by short filaments in an apparent depot close to the sites of calcium influx (Lenzi et al. 1999). Vesicles attached to the synaptic ribbon of the rod bipolar cells define a functional pool of "readily releasable vesicles" (von Gersdorff et al. 1996), and depletion of these vesicles from the ribbon is thought to contribute to synaptic depression (von Gersdorff and Matthews 1997).

The cochlea must encode information about the amplitude, duration, and frequency of the acoustic stimulus. The continuous nature of acoustic signals requires that the hair cell synapse sustain the release of neurotransmitter for prolonged periods of time. Such high-frequency firing can persist unabated for several minutes (Kiang 1965). The temporal demands of the auditory system are also remarkable. Two examples of the hair cell's exquisite dependency on phasic signaling occur with sound localization and periodicity pitch. Minute differences (10's of μs) in the arrival of acoustic waves at each ear are used by higher centers in the brain for azimuthal sound localization (Moiseff and Konishi 1981). Pitch recognition of certain frequency sounds such as "the missing fundamental" (de Boer 1976; Schouten 1940) is limited by the ability the hair cell synaptic output to maintain a preferred phase angle between individual cycles of an acoustic stimuli and afferent fiber discharges. Depending on the species, the ability of an afferent fiber to phase-lock to an acoustical signal fails between 0.9 kHz (frog: Hillery and Narins 1987) and 9.0 kHz (barn owl: Koppl 1997; Sullivan and Konishi 1984). Thus hearing requires the hair cell synapse to maintain notable temporal fidelity (≤1 ms) while sustaining neurotransmitter release for prolonged periods of time (minutes).

Auditory nerve discharge rates adapt in response to continuous pure tone stimulation (Kiang 1965). A decrement in the release of neurotransmitter by the hair cell has been suggested to underlie auditory nerve adaptation (Furukawa et al. 1982; Moser and Beutner 2000). Our studies in the chick basilar papilla (avian equivalent of the mammalian cochlea) of both hair cell exocytosis and eighth nerve single-unit recordings support this notion (Spassova et al., unpublished observations). Sound-evoked afferent synaptic activity adapted and recovered with similar time courses as readily releasable pool exhaustion and recovery. Comparison of the readily releasable pool size and number of vesicles tethered to the synaptic ribbon suggested that the readily releasable pool is defined by vesicles tethered to the synaptic ribbons. However, longer depolarizations yielded a second, slower, sustained kinetic component of exocytosis.

Here we probed the properties and possible anatomical substrate of prolonged neurotransmitter release by using electrical measures of cell surface area as a proxy for neurotransmitter release to study hair cell exocytosis evoked by repetitive stimuli. We observed marked depression of exocytosis by chick auditory hair cells. We attribute this depression to the exhaustion of a functional vesicle pool. Such a large functional pool suggests the recruitment of cytoplasmic vesicles to sustain exocytosis and maintain prolonged, high rates of neural activity needed to encode sound.

METHODS

The methods used here are similar to those reported previously (Spassova et al. 2001) and will be described in brief.

Address for reprint requests and other correspondence: T. D. Parsons, Department of Clinical Studies, New Bolton Center, University of Pennsylvania School of Veterinary Medicine, 382 West Street Rd., Kennett Square, PA 19348 (E-mail: thd@vet.upenn.edu).

The costs of publication of this article were defrayed in part by the payment of page charges. The article must therefore be hereby marked "*advertisement*" in accordance with 18 U.S.C. Section 1734 solely to indicate this fact.

Tissue preparation

Cochlear capsules were harvested (Zidanic and Fuchs 1995) from 7- to 12-day-old white leghorn chicks (*Gallus domesticus*) following a protocol approved by the IACUC of the University of Pennsylvania. The sensory epithelium was removed, and a section of the sensory epithelium approximately 400 μm long, starting 0.5 mm from the apical tip of the basilar papilla, was mounted in a recording chamber. To minimize any possible confounding effects of tonotopy (Martinez-Dunst et al. 1997), our patch-clamp recordings were limited to the neural-most tall hair cells located approximately 0.5 to 1.0 mm from the apical end of the basilar papilla [corresponding to frequencies around 200 Hz (Manley et al. 1996)]. The basolateral surface of the neural-most individual tall hair cells was visualized with an upright, fixed-stage compound microscope. The recording chamber contained the control external saline (in mM: 154 NaCl, 6 KCl, 5 HEPES, 8 glucose, 2 $MgCl_2$, 5 $CaCl_2$, pH balanced to 7.4 with NaOH) (Fuchs et al. 1988).

Whole cell patch-clamp recording

Individual tall hair cells were patch clamped using tight seal recordings in whole cell configuration (Hamill et al. 1981). Cells were voltage-clamped at a holding potential of −81 mV with either an Axopatch 200B (Axon Instruments, Foster City, CA) or an EPC9 patch-clamp amplifier (HEKA Electronics GmbH, Lambrecht, Germany). A mean resting membrane capacitance of 6.1 ± 0.2 pF (n = 56) was recorded from tall hair cells by a mean access resistance 8.9 ± 0.3 MΩ (n = 56). Pipettes (KIMAX 51, World Precision Instruments) were coated with purple ski wax (SWIX, Lillehammer, Norway) to reduce their capacitance, and filled with the control internal solution [in mM: 115 glutamic acid, 115 CsOH, 20 tetraethylammonium (TEA) chloride, 13 NaCl, 10 HEPES, 3 MgCl, 5 Na-ATP, 0.3 GTP, 0.2 EGTA, pH balanced with CsOH to 7.4]. A liquid junction potential of +11 mV was measured for our cesium glutamate internal solution (Spassova et al. 2001), and all voltages are corrected by subtraction of this liquid junction potential.

Changes in cell membrane capacitance (ΔC_m) were used to monitor fusion of neurotransmitter-containing vesicles during exocytosis, and measured with either the "piecewise linear" technique with a dual lock-in amplifier (H. Meyer, Goettingen, Germany) (Gillis 1995; Lindau and Neher 1988) or by the "sine+DC" mode of the EPC-9 software lock-in amplifier (Gillis 2000). Either an 800-Hz (40 mV peak-to-peak) or a 1.25-kHz (25 mV peak-to-peak) sinusoidal command voltage was superimposed on the holding potential of −81 mV. Hair cell excytosis was elicited by trains of 4–10 depolarizing voltage-clamp steps to −21 mV that ranged in duration from 0.3 to 3.0 s at 6-s intervals. Calcium currents were sampled at 50-μs intervals, filtered at 2.9 kHz. Capacitance data were filtered and analyzed off-line using IgorPro software (Wavemetrics, Lake Oswego, OR) or Microsoft Excel (Microsoft, Redwood, WA).

Data analysis

All experiments were done at 20–22°C, and all measurements are given as mean values ± 1 SE unless otherwise stated. Values of ΔC_m elicited by each depolarization were quantified as the difference between the average value of a 200-ms C_m segment immediately before the depolarization and one measured 400 ms after the end of the depolarizing pulse. This avoided any contamination of the exocytotic response by capacitive transients not associated with exocytosis (Debus et al. 1995; Horrigan and Bookman 1994).

An alternative to the repeated-measures ANOVA, the generalized estimating equations, was used to compare the successive ΔC_m values of the CPPG-treated versus control cells because it accounts for the dependency of successive ΔC_m values for a given cell (Zeger and Liang 1986). The ΔC_m data were fitted to the finite pool model with a least-squares algorithm (TableCurve 2D, Systat Software, Richmond, CA), and how well the model explained data variance was assessed with the R^2 statistic. The number of available capacitance data points ranged from 4 to 10 per cell and all the available data for each cell were used in the fitting procedure. The dependency of B_0 on pulse length was tested with a simple linear regression model (Sigmaplot, SPSS, Chicago, IL).

Estimate of pool size

The number of vesicles in the releasable pool was calculated by dividing ΔC_m by the estimated single-vesicle capacitance reported in an anatomical study on the bullfrog saccular hair cell (Lenzi et al. 1999). This single-vesicle capacitance of 37 aF was derived using a specific capacitance of membrane as 1 $\mu F/cm^2$ and a mean vesicle diameter of 34.3 nm. A similar mean vesicle diameter was found when we measured a sample of the vesicles found in the published electron micrograph of chick cochlear hair cells taken from the same approximate location on the basilar papilla as cells in our experiments (Martinez-Dunst et al. 1997).

RESULTS

Prolonged cochlear hair cell exocytosis triggered by repetitive depolarization

Hair cell depolarization induces a membrane capacitance jump attributed to the calcium-dependent increase in cell surface area associated with fusion of synaptic vesicles preceding neurotransmitter release (Beutner et al. 2001; Moser and Beutner 2000; Parsons et al. 1994; Spassova et al. 2001). Repeated stimulation of the chick cochlear hair cell with identical depolarizations spaced 6 s apart results in a series of steplike capacitance increases (Fig. 1*A*). However, each subsequent exocytic response in the train is smaller than the previous. The extent of the exocytic depression in Fig. 1*A* is quantified by measuring each subsequent capacitance jump (Fig. 1*B*). The amplitude of subsequent ΔC_m decays over the course of 2 to 4 stimuli and reaches a constant, but nonzero, value during the train of depolarizing stimuli. On average, the ΔC_m response to depolarizing stimulus trains behaved similarly (Fig. 1*C*). The first pulse in the train elicited a mean ΔC_m of 194 ± 20 fF (n = 29). Subsequent ΔC_m progressively decreased and ultimately approached a constant value of 15 ± 2 fF per pulse. This 13-fold activity-dependent decrement of exocytosis is reminiscent of synaptic depression, a common form of synaptic plasticity after repeated activation of the nerve terminal (Betz 1970; Zucker 1989).

Our studies of membrane capacitance reveal synaptic depression that can only be presynaptic in origin, thus demonstrating that postsynaptic processes such as receptor desensitization and saturation might further contribute to cochlear hair cell-afferent plasticity, but are not required. Possible presynaptic mechanisms underlying exocytic depression at this synapse are tested here.

Direct recording of calcium influx by voltage-dependent calcium channels (Fuchs et al. 1990; Hudspeth and Lewis 1988) allow us to test whether I_{Ca} inactivation is the cause of the observed exocytic depression. Figure 2*A* shows I_{Ca} current activated by a train of 7 depolarizations to −21 mV. In this cell, no decrease in the amplitude of the current was observed between subsequent pulses as I_{Ca} remained constant throughout the train at −97.1 ± 0.8 pA (n = 7 pulses). As in other

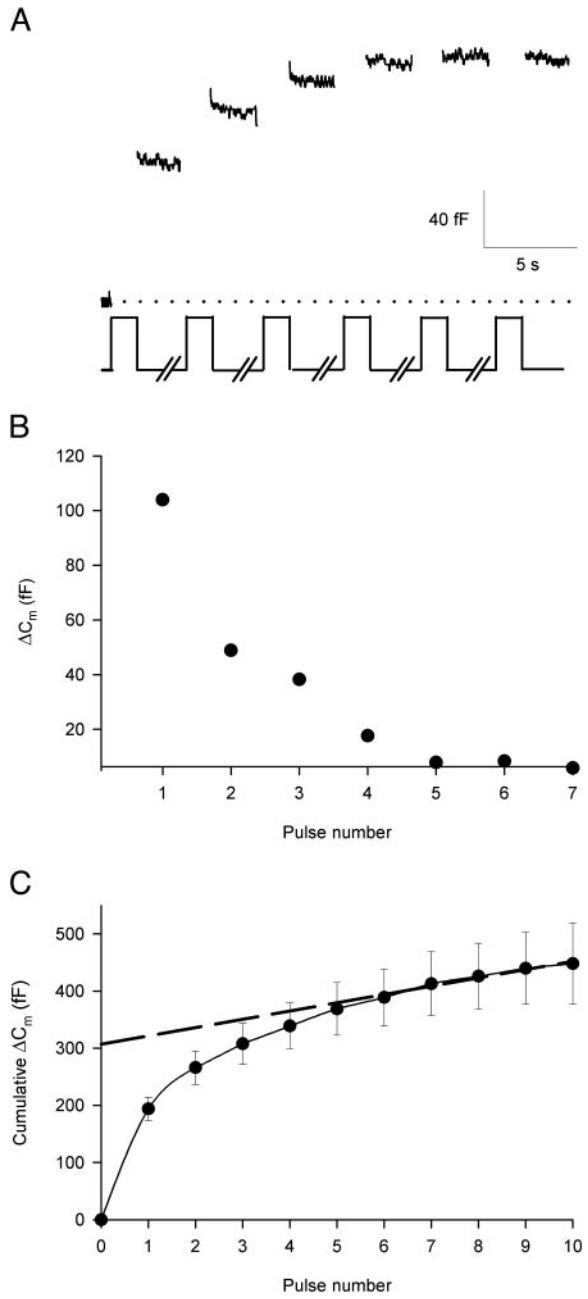

FIG. 1. Repeated depolarization results in cochlear hair cell exocytic depression. *A*: cell membrane capacitance increases triggered by a train of 0.5-s depolarizations spaced 6 s apart. Membrane is depolarized from a holding potential of −81 to −21 mV to activate calcium channels and maximally stimulate exocytosis (Spassova et al. 2001). *B*: magnitude of ΔC_m calculated for the cell in *A* for each successive pulse. *C*: average membrane capacitance increases from 29 cells following train stimuli. Line fitted to last 5 data points has a slope of 15 ± 2 fF per pulse and a *y*-intercept of 307 ± 13 fF.

cells studied, no significant calcium channel inactivation develops during the individual test pulse of the train (Fig. 2*B*). Consistent with the observations here, hair cell I_{Ca} is characterized as both rapidly activating and deactivating, and noninactivating (Fuchs et al. 1990; Hudspeth and Lewis 1988; Rodriguez-Contreras et al. 2002; Zidanic and Fuchs 1995), and thus does not account for the exocytic depression.

Activation of presynaptic metabotropic glutamate receptors (mGluR) contribute, at least in part, to declining responses to repeated stimulation of glutamatergic CNS synapses (Scanziani et al. 1997; von Gersdorff et al. 1997). These receptors are present and functional in some hair cells (Guth et al. 1993; Hendricson and Guth 2002a,b), and thus repeated one-second depolarizations were given in the presence and absence of (RS)-a-cyclopropyl-4-phosphono-phenylglycine (CPPG), a potent antagonist of presynaptic mGlu receptors (Jane et al. 1996) (Fig. 2*C*). If presynaptic mGluR activation was responsible for declining ΔC_m, then exposure to a mGLuR antagonist is predicted to alleviate the exocytic depression. However, statistical analysis of exocytic depression in the presence of 300 μM CPPG ($n = 5$ cells) showed no difference from that in control cells ($n = 7$ cells; $P = 0.17$).

The exocytic depression could be secondary to the washout of a factor or factors mediating exocytosis over the time period of the recording (Hay and Martin 1992; Moser and Beutner 2000; Neves and Lagnado 1999). To test this notion, we examined the ability of the hair cell exocytic depression to recover. The standard train of stimuli was applied to depress exocytosis, and then a variable interval was allowed before a single test stimulus was delivered. The ratio of the test pulse to the first pulse of the conditioning train is plotted in Fig. 2*D*. Over 60% of the initial ΔC_m is recovered within 1.5 min of the end of the train. This slow recovery time course after trains of depolarization is similar to the retinal bipolar cell ribbon synapse where 100 s or longer is required for recovery (von Gersdorff and Matthews 1997). The lack of complete recovery may be attributable to the rundown or washout of exocytic capacity over a time course of many minutes. However, a major portion of exocytosis recovers after a depressing stimulus train and suggests that exocytic rundown does not explain the exocytic depression observed during an approximately 50-s stimulus train.

Large pool of releasable vesicles

Having ruled out several possible mechanisms of depression, we hypothesized that the diminishing exocytic response results from the exhaustion of a finite releasable vesicle population (Neher 1998; Schneggenburger et al. 2002). A simple model was developed to test this hypothesis. Given a finite releasable vesicle pool with size B_0 and α, the fraction of vesicles available for release, then ΔC_m is predicted as $B_0 \times \alpha$. Alternatively, pairs of successive ΔC_m values can be used to determine B_0 if α is similar from stimulation to stimulation (Gillis et al. 1996).

The hair cell exocytotic responses to repeated depolarizations followed an apparently exponential decay (see Fig. 3*A*), consistent with a constant release fraction α during successive pulses. Therefore we extended the Gillis–Neher formalism to determine the initial pool size using the ΔC_m of successive depolarizations of the stimulus train. In addition to B_0 and α, the model also included a constant R, which is interpreted as the amount of pool refilled in between stimuli. Successive ΔC_m magnitudes would be expected to yield a geometric series having the following form (see APPENDIX for derivation)

$$\Delta C_n = (1 - \alpha)^{n-1}(\alpha B_0 - R) + R \quad (1)$$

where ΔC_n is the capacitance change in fF associated with the *n*th pulse.

The ΔC_m values predicted by the model (solid line in Fig. 3*A*)

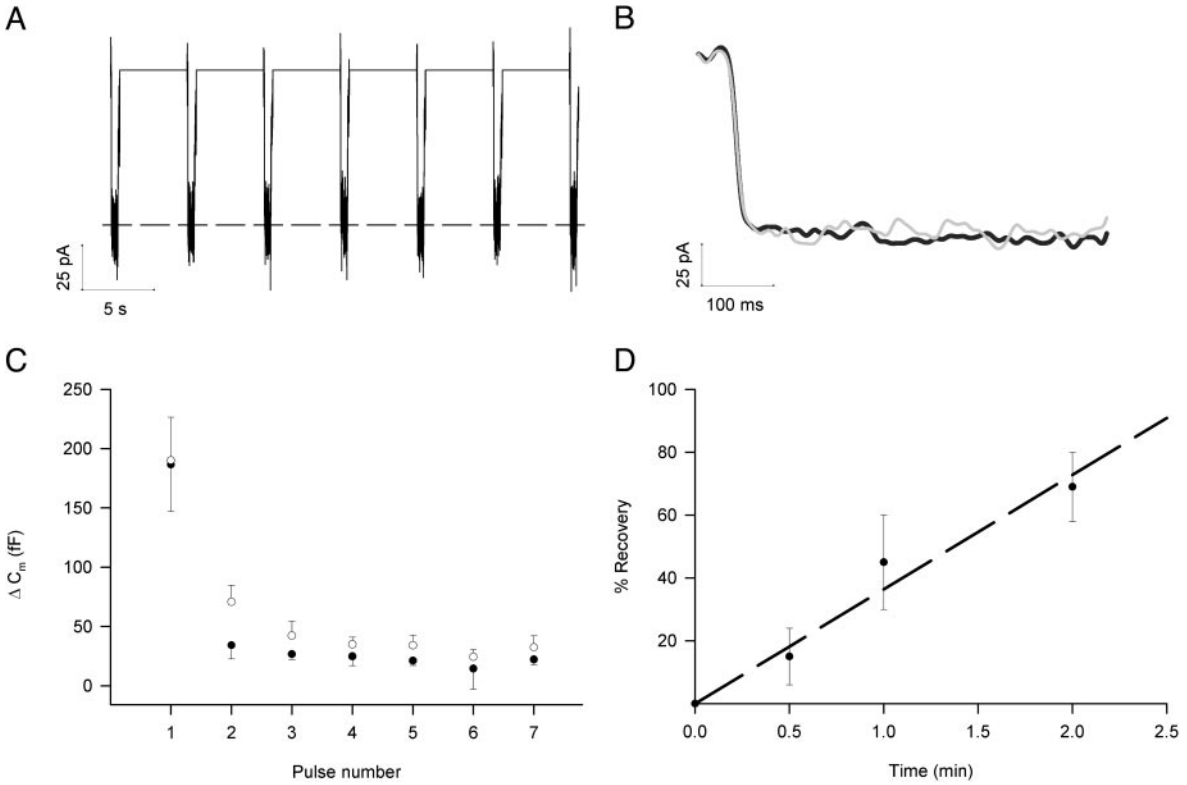

FIG. 2. Possible mechanisms of exocytic depression. *A*: calcium current inactivation not responsible for exocytic depression. Calcium currents elicited with repeated 0.5-s depolarizations, similar to Fig. 1. *B*: time-expanded view of first and last 0.5-s depolarization. *C*: presynaptic metabotropic glutamate receptors do not contribute to the exocytic depression. Cells were given repeated 1-s depolarizing stimuli from a holding potential of −81 to −21 mV every 6 s in the presence (solid circles; $n = 5$) or absence (open circles; $n = 7$) of the mGluR antagonist CPPG (300 μM). *D*: recovery from exocytic depression. Percentage recovery is plotted vs. time between the end of the depressing stimulus train (0.5-s depolarizing steps from −81 to −21 mV every 6 s) and the test pulse of 0.5 s. Recovery of exocytosis proceeds in linear fashion at a rate of 0.5%/s, but complete recovery was not achieved during the time course of these experiments.

correlated well with the experimental observations. In this example, the model fit with an R^2 of 0.95 and yielded a value of 0.44 for α, whereas $B_0 = 300$ fF and $R = 24$ fF. Values of α varied widely between cells (range: 0.23 and 0.96; mean 0.64 ± 0.04; $n = 29$). However, the fit of the model to the data remained robust ($R^2 > 0.75$) over this wide variation of α (Fig. 3*B*).

Given the good fit of our finite pool model to the data, we then estimated the pool size of synaptic vesicles that support prolonged exocytosis. The pool of vesicles available before each stimulus was determined by dividing ΔC_{n+1} by α. The mean value of B_0, the initial pool, using this method was 311 ± 33 fF ($n = 29$ cells) and corresponds to approximately 8,000 synaptic vesicles (see METHODS). B_0 was independent of both pulse duration (Table 1) and the fractional release per pulse α (Fig. 3*C*), further validating the appropriateness of the finite pool model. The mean value for the constant R was 18.7 ± 3.3 fF per pulse, or 3.1 fF/s. This was similar to the 15.0 ± 2.0 fF per pulse slope of the asymptote fitted to the average ΔC_m data in Fig. 1*C*. Given a pool size of approximately 310 fF and a refilling rate of approximately 3 fF/s, then nominally 100 s would be required to refill the large releasable pool. Thus these estimates of R are consistent with the 90- to 120-s exocytic recovery time measured after a train of depolarizations (see Fig. 2*D*).

The B_0 value predicted by the finite pool model was similar to the initial pool size of 307 ± 13 fF described by the *y*-intercept of the asymptote fitted to the average ΔC_m data in Fig. 1*C*. Furthermore, the original algorithm described by Gillis et al. (1996) to determine α with a pair of pulses also yielded a similar value for pool size. Because α was not assumed to be constant for successive pulses, an upper limit of B_0 (B_{max}) was determined, which was equal to B_0 when the fractional release of the first pulse equaled that of the second. In the hair cell, the paired-pulse algorithm yielded a value for B_{max} of 307 ± 30 fF ($n = 42$). The data used for the paired-pulse analysis include the first 2 pulses from the 29 cells fitted to the finite pool model. None of these 3 estimates of initial pool size is significantly different from the other ($P > 0.05$). Thus 3 different estimates of B_0 yielded approximately 8,000 vesicles. The correspondence between the first 2 measures of initial pool size with the prediction of paired-pulse algorithm is important, given that the latter estimate does not share any assumptions about α or R. Taken together these observations support the hypothesis that a large finite releasable vesicle population mediates prolonged exocytosis after repetitive stimulation of the cochlear hair cell.

DISCUSSION

Functional versus anatomical pools of vesicles

The concept of functional pools of releasable or available vesicles at a synapse is well established (Neher 1998). These pools vary in both size and number, and likely serve different

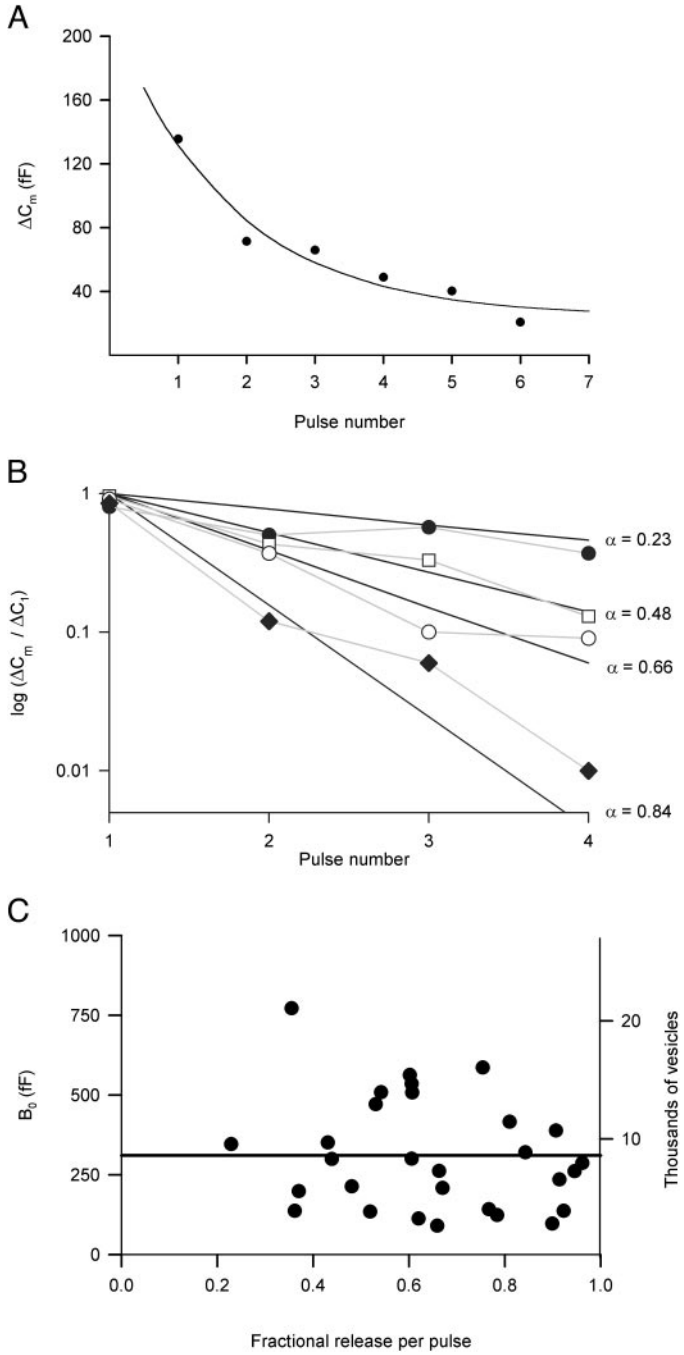

FIG. 3. Depression of ΔC_m allows for calculation of releasable pool size. *A*: magnitude of ΔC_m calculated for another cell as in (Fig. 1*B*) for each successive pulse and then fit with model. *B*: model used to predict B_0 is robust over large range of α. Shown are the normalized ΔC_m of the first 4 pulses of 4 representative cells (symbols) on a log scale after subtracting the parameter R from each value. Solid line is the model prediction for each cell and shows a good fit for a range of fractional release values. *C*: fractional release per pulse (α) plotted vs. the initial releasable pool size (B_0) shows no correlation between the two parameters. Solid line represents that average value of B_0. Values of ΔC_m were converted to a number of vesicles (see METHODS for details of calculation) and shown on the right-hand axis. Of 39 cells given repetitive stimuli, the successive ΔC_m from 33 that yielded $\Delta C_1 > \Delta C_2$ were subjected to analysis by a model that assumed a constant fractional release per pulse (α) (see *Eq. 1*). Data from 29 of these 33 cells fit the model with an $R^2 > 0.75$, and these were used to determine the initial releasable pool size, B_0.

functions at different synapses. Perhaps the best-studied example is the rod bipolar cell of the goldfish retina. There, a readily releasable pool of approximately 6,000 vesicles has been identified (von Gersdorff and Matthews 1994), and mediates the fast transient release of glutamate (von Gersdorff et al. 1998). Because the size of this functional pool corresponds to anatomical measures of the number of vesicles attached to the rod bipolar cell synaptic ribbons, the two are thought to be equivalent (von Gersdorff et al. 1996).

We recently described (Spassova et al., unpublished observations) a readily releasable pool in chick cochlear hair cells that is similarly defined by the vesicles tethered to the synaptic ribbon. This pool contains only about 1,000 vesicles because of the small number and size of synaptic ribbons in chick hair cells (Martinez-Dunst et al. 1997). The experimental protocols used in this report, however, lack sufficient temporal resolution to specifically discern the contribution of readily releasable vesicles to the functional pool identified here that is exhausted by trains of stimuli. This large releasable pool is 8 times the size of the readily releasable pool, and thus is too big to be accounted for by vesicles tethered to the ribbon. Therefore we suggest that the large releasable pool described here consists, in part, of vesicles tethered to the synaptic ribbon, but primarily of vesicles recruited from the cytoplasm.

This pool may be the anatomical basis of the slow component of chick hair cell exocytosis that mediates reloading of the ribbon with vesicles (Spassova et al., unpublished observations). However, the large pool described here is still only a fraction of either the 45,000 release competent vesicles reported in mouse cochlear hair cells (Beutner et al. 2001) or the $2–6 \times 10^5$ total synaptic vesicles in the frog saccular hair cell (Lenzi et al. 1999). Even given quantitative differences in the presynaptic ultrastructure of different hair cells, the releasable pool defined in this report is sufficiently small compared with these other vesicle counts to argue that the pool consists of only a subset of cytoplasmic vesicles. What defines this subset of hair cell synaptic vesicles as releasable remains unclear. Calcium has been asserted at other synapses to play a role in vesicle recruitment (Sakaba and Neher 2001; Wang and Kaczmarek 1998; Wu and Borst 1999). Mouse cochlear hair cells exhibited a sustained secretory component that depended on intracellular calcium buffering (Moser and Beutner 2000), and may be supported by mechanisms common to our large releasable pool. We used 0.2 mM EGTA as the pipette calcium buffer, which is similar to the equivalent endogenous buffer in the mouse hair cell as well as permissive for the sustained secretory component. Other mechanisms proposed to mobilize or recruit synaptic vesicles to release sites at different synapses remain controversial, but may involve actin cortices (Job and Lagnado 1998; Sakaba and Neher 2003), synapsin (Chi et al.

TABLE 1. *B_0 is independent of pulse duration*

Pulse Duration, ms	Pool Size, fF	*N*
300	292 ± 96	3
500	252 ± 58	4
1,000	319 ± 61	12
1,500	261 ± 88	4
3,000	377 ± 67	6

Simple linear regression analysis did not reveal a statistically significant relationship between pulse length and pool size ($P = 0.33$).

2001; Farve et al. 1986; Hilfiker et al. 1998), and/or molecular motors (Griesinger et al. 2002; Heidelberger et al. 2003; Mochida et al. 1994; Ryan 1999).

Relevance of large releasable pool to hair cell function

Hair cell afferent synapses exhibit exceptional phasic and tonic neurotransmitter release. Comparison of readily releasable pool kinetics in chick cochlear hair cells with single-unit recordings of cochlear nerve in the same species suggest that adaptation of nerve discharge is mediated by synaptic vesicles tethered to the synaptic ribbons (Spassova et al., unpublished observations). However, the adapted nerve fiber continues to fire for seconds and minutes if the stimulus is maintained, and this ability to sustain prolonged neurotransmitter release requires a large number of available vesicles, presumably supplied by the functional pool described here. The ample supply of synaptic vesicles also ensures that transmitter release is both reliable and timely, even given inherently slow exocytic processes (Almers 1994). Thus the existence of a large releasable pool is likely critical to both phasic and tonic neurotransmitter release by cochlear hair cells.

We estimated this pool size based on membrane capacitance measurement, which is the net sum of exo- and endocytosis. Our previous work on bullfrog saccular hair cells has shown that whole cell patch-clamp recording blocks endocytosis presumably attributable to the washout of critical factors (Parsons et al. 1994). This is in contrast to studies on mouse inner hair cells where whole cell recording conditions were less favorable for cytoplasmic exchange, and endocytosis was observed (Moser and Beutner 2000). Although we see no evidence of endocytosis in our measurements on chick cochlear hair cells, we cannot, however, formally exclude that possibility. If endocytosis is ongoing during the pulse, then our measures are actually underestimates of the size of the large functional pool needed to sustain prolonged exocytosis.

In conclusion, a large functional pool of synaptic vesicles maintains prolonged hair cell exocytosis evoked by repetitive stimulation. This functional pool is almost 10-fold larger than the number of vesicles that are found on the synaptic ribbon, and differs from what has been reported in the retinal bipolar cell. There the releasable pool evoked under similar stimulation conditions is not more than twice the size of the vesicles tethered to the ribbons (von Gersdorff and Matthews 1997; von Gersdorff et al. 1996). Apparently the sustained demands on neurotransmitter release placed by hearing require specialized mechanisms that allow a large number of cytoplasmic vesicles to rapidly participate in exocytosis. We also observed that both the exhaustion and refilling of chick hair cell readily releasable pool is as much as 10 times faster (Spassova et al., unpublished observations) than comparable measures in the retinal bipolar cells. Taken together these observations further reinforce the existence of fundamental differences between ribbon synapses in the auditory and visual systems.

APPENDIX: DERIVING CALCULATION OF INITIAL RELEASABLE POOL SIZE

Definition of variables

B_0 = initial pool size (in fF)
B_n = Pool size before the $(n + 1)$th depolarization (in fF)
ΔC_n = capacitance change after the nth depolarization (in fF)
R = constant ΔC_m per pulse (fF/pulse)
α = fraction of the available pool released during each pulse

Multiple depolarizations

Any depolarization yields the capacitance change ΔC_{n+1} by the equation

$$\Delta C_{n+1} = \alpha B_n \quad (A1)$$

The pool size before the nth depolarization, given a refilling of R (fF/pulse), is then

$$B_n = (1 - \alpha)B_{n-1} + R \quad (A2)$$

Subtracting R/α from each side of *Eq. A2*, and rearranging, yields

$$B_n - R/\alpha = (1 - \alpha)(B_{n-1} - R/\alpha) \quad (A3)$$

By induction

$$B_n - R/\alpha = (1 - \alpha)^n(B_0 - R/\alpha) \quad (A4)$$

By substituting *Eq. A1* one obtains

$$\Delta C_{n+1} = (1 - \alpha)^n(\alpha B_0 - R) + R \quad (A5)$$

This equation can be fit using the capacitance changes associated with multiple depolarizations to determine α, B_0, and R.

ACKNOWLEDGMENTS

We thank G. Ellis-Davies for the use of equipment, A. Mitelman for mathematical advice, and J. C. Saunders for helpful discussions and continued support.

GRANTS

This work was funded by National Institute on Deafness and Other Communication Disorders Grant DC-03763 and a Sloan Research Fellowship.

REFERENCES

Almers W. Synapses. How fast can you get? *Nature* 367: 682–683, 1994.
Betz WJ. Depression of transmitter release at the neuromuscular junction of the frog. *J Physiol* 206: 629–644, 1970.
Beutner D, Voets T, Neher E and Moser T. Calcium dependence of exocytosis and endocytosis at the cochlear inner hair cell afferent synapse. *Neuron* 29: 681–690, 2001.
Chi P, Greengard P and Ryan TA. Synapsin dispersion and reclustering during synaptic activity. *Nature Neuroscience* 4: 1187–1193, 2001.
de Boer, E. On the residue hearing and auditory pitch perception. In: *Handbook of Sensory Physiology*: *Auditory System*, edited by Keidel WD and Neff WD. Berlin: Springer-Verlag, vol. 5, p. 479–584, 1976.
Debus K, Hartmann J, Kilic G, and Lindau M. Influence of conductance changes on patch clamp capacitance measurements using a lock-in amplifier and limitations of the phase tracking technique. *Biophys J* 69: 2808–2822, 1995.
Farve D, Scarfone E, Di Gioia G, De Camilli P, and Dememes D. Presence of synapsin I in afferent and efferent nerve endings of vestibular sensory epithelia. *Brain Res* 384: 379–382, 1986.
Fuchs PA, Evans MG, and Murrow BW. Calcium currents in hair cells isolated from the cochlea of the chick. *J Physiol* 429: 553–568, 1990.
Fuchs PA, Nagai T, and Evans MG. Electrical tuning in hair cells isolated from the chick cochlea. *J Neurosci* 8: 2460–2467, 1988.
Furukawa T, Kuno M, and Matsuura S. Quantal analysis of a decremental response at hair cell-afferent fibre synapses in the goldfish sacculus. *J Physiol* 322: 181–195, 1982.
Gillis AM, Fast VG, Rohr S, and Kleber AG. Spatial changes in transmembrane potential during extracellular electrical shocks in cultured monolayers of neonatal rat ventricular myocytes. *Circ Res* 79: 676–690, 1996.
Gillis K. Techniques for membrane capacitance measurements. In: *Single-Channel Recording* (2nd ed.), edited by Sakmann B and Neher E. New York: Plenum, 1995, p. 155–198.

Gillis KD. Admittance-based measurement of membrane capacitance using the EPC-9 patch-clamp amplifier. *Pflügers Arch* 439: 655–664, 2000.

Griesinger CB, Richards CD, and Ashmore JF. Fm1–43 reveals membrane recycling in adult inner hair cells of the mammalian cochlea. *J Neurosci* 22: 3939–3952, 2002.

Guth P, Norris C, Fermin CD, and Pantoja M. The correlated blanching of synaptic bodies and reduction in afferent firing rates caused by transmitter-depleting agents in the frog semicircular canal. *Hear Res* 66: 143–149, 1993.

Hamill OP, Marty A, Neher E, Sakmann B, and Sigworth FJ. Improved patch-clamp techniques for high-resolution current recording from cells and cell-free membrane patches. *Pflügers Arch* 391: 85–100, 1981.

Hay JC and Martin TF. Resolution of regulated secretion into sequential MgATP-dependent and calcium-dependent stages mediated by distinct cytosolic proteins. *J Cell Biol* 119: 139–151, 1992.

Heidelberger R, Sterling P, and Matthews G. Role of ATP in depletion and replenishment of the releasable pool of synaptic vesicles. *J Neurophysiol* 88: 2509–2517, 2003.

Hendricson AW and Guth PS. Signal discrimination in the semicircular canals: a role for group I metabotropic glutamate receptors. *Neuroreport* 13: 1765–1768, 2002a.

Hendricson AW and Guth PS. Transmitter release from *Rana pipiens* vestibular hair cells via mGluRs: a role for intracellular Ca(++) release. *Hear Res* 172: 99–109, 2002b.

Hilfiker S, Schweizer FE, Kao HT, Czernik AJ, Greengard P, and Augustine GJ. Two sites of action for synapsin domain E in regulating neurotransmitter release [erratum appears in Nat Neurosci 1998 Aug;1(4): 329]. *Nat Neurosci* 1: 29–35, 1998.

Hillery CM and Narins PM. Frequency and time domain comparison of low-frequency auditory fiber responses in two anuran amphibians. *Hear Res* 25: 233–248, 1987.

Horrigan FT and Bookman RJ. Releasable pools and the kinetics of exocytosis in adrenal chromaffin cells. *Neuron* 13: 1119–1129, 1994.

Hudspeth AJ and Lewis RS. Kinetic analysis of voltage- and ion-dependent conductances in saccular hair cells of the bull-frog, *Rana catesbeiana*. *J Physiol* 400: 237–274, 1988.

Issa NP and Hudspeth AJ. Clustering of Ca^{2+} channels and Ca(2+)-activated K^+ channels at fluorescently labeled presynaptic active zones of hair cells. *Proc Natl Acad Sci USA* 91: 7578–7582, 1994.

Jane DE, Thomas NK, Tse HW, and Watkins JC. Potent antagonists at the L-AP4- and (1S,3S)-ACPD-sensitive presynaptic metabotropic glutamate receptors in the neonatal rat spinal cord. *Neuropharmacology* 35: 1029–1035, 1996.

Job C and Lagnado L. Calcium and protein kinase C regulate the actin cytoskeleton in the synaptic terminal of retinal bipolar cells. *J Cell Biol* 143: 1661–1672, 1998.

Kiang NYS. *Discharge Patterns of Single Fibers in the Cat's Auditory Nerve*. Cambridge, MA: MIT Press, 1965.

Koppl C. Phase locking to high frequencies in the auditory nerve and cochlear nucleus magnocellularis of the barn owl, *Tyto alba*. *J Neurosci* 17: 3312–3321, 1997.

Lenzi D, Runyeon JW, Crum JW, Ellisman MH, and Roberts WM. Synaptic vesicle populations in saccular hair cells reconstructed by electron tomography. *J Neurosci* 19: 119–132, 1999.

Lenzi D and von Gersdorff H. Structure suggests function: the case for synaptic ribbons as exocytotic nanomachines. *Bioessays* 23: 831–840, 2001.

Lindau M and Neher E. Patch-clamp techniques for time-resolved capacitance measurements in single cells. *Pflügers Arch* 411: 137–146, 1988.

Manley GA, Meyer B, Fischer FP, Schwabedissen G, and Gleich O. Surface morphology of basilar papilla of the tufted duck *Aythya fuligula*, and domestic chicken *Gallus gallus domesticus*. *J Morphol* 227: 197–212, 1996.

Martinez-Dunst C, Michaels RL, and Fuchs PA. Release sites and calcium channels in hair cells of the chick's cochlea. *J Neurosci* 17: 9133–9144, 1997.

Mochida S, Kobayashi H, Matsuda Y, Yuda Y, Muramoto K, and Nonomura Y. Myosin II is involved in transmitter release at synapses formed between rat sympathetic neurons in culture. *Neuron* 13: 1131–1142, 1994.

Moiseff A and Konishi M. Neuronal and behavioral sensitivity to binaural time differences in the owl. *J Neurosci* 1: 40–48, 1981.

Moser T and Beutner D. Kinetics of exocytosis and endocytosis at the cochlear inner hair cell afferent synapse of the mouse. *Proc Natl Acad Sci USA* 97: 883–888, 2000.

Nachman-Clewner M, St Jules R, and Townes-Anderson E. L-type calcium channels in the photoreceptor ribbon synapse: localization and role in plasticity. *J Comp Neurol* 415: 1–16, 1999.

Neher E. Vesicle pools and Ca^{2+} microdomains: new tools for understanding their roles in neurotransmitter release. *Neuron* 20: 389–399, 1998.

Neves G and Lagnado L. The kinetics of exocytosis and endocytosis in the synaptic terminal of goldfish retinal bipolar cells. *J Physiol* 515: 181–202, 1999.

Parsons TD, Lenzi D, Almers W, and Roberts WM. Calcium-triggered exocytosis and endocytosis in an isolated presynaptic cell: capacitance measurements in saccular hair cells. *Neuron* 13: 875–883, 1994.

Parsons TD and Sterling P. Synaptic ribbon: conveyor belt or safety belt? *Neuron* 37: 379–382, 2003.

Roberts WM, Jacobs RA, and Hudspeth AJ. Colocalization of ion channels involved in frequency selectivity and synaptic transmission at presynaptic active zones of hair cells. *J Neurosci* 10: 3664–3684, 1990.

Rodriguez-Contreras A, Nonner W and Yamoah EN. Ca^{2+} transport properties and determinants of anomalous mole fraction effects of single voltage-gated Ca^{2+} channels in hair cells from bullfrog saccule. *J Physiol* 538: 729–745, 2002.

Ryan TA. Inhibitors of myosin light chain kinase block synaptic vesicle pool mobilization during action potential firing. *J Neurosci* 19: 1317–1323, 1999.

Sakaba T and Neher E. Quantitative relationship between transmitter release and calcium current at the calyx of held synapse. *J Neurosci* 21: 462–476, 2001.

Sakaba T and Neher E. Involvement of actin polymerization in vesicle recruitment at the calyx of Held synapse. *J Neurosci* 23: 837–846, 2003.

Scanziani M, Salin PA, Vogt KE, Malenka RC and Nicoll RA. Use-dependent increases in glutamate concentration activate presynaptic metabotropic glutamate receptors. *Nature* 385: 630–634, 1997.

Schneggenburger R, Sakaba T, and Neher E. Vesicle pools and short-term synaptic depression: lessons from a large synapse. *Trends Neurosci* 25: 206–212, 2002.

Schouten J. The residue and the mechanism of hearing. *Proc Koninkl Nederland Akad Wetensch* 43: 991–999, 1940.

Spassova M, Eisen MD, Saunders JC, and Parsons TD. Chick cochlear hair cell exocytosis mediated by dihydropyridine-sensitive calcium channels. *J Physiol* 535: 689–696, 2001.

Sullivan WE and Konishi M. Segregation of stimulus phase and intensity coding in the cochlear nucleus of the barn owl. *J Neurosci* 4: 1787–1799, 1984.

von Gersdorff H. Synaptic ribbons: versatile signal transducers. *Neuron* 29: 7–10, 2001.

von Gersdorff H and Matthews G. Dynamics of synaptic vesicle fusion and membrane retrieval in synaptic terminals. *Nature* 367: 735–739, 1994.

von Gersdorff H and Matthews G. Depletion and replenishment of vesicle pools at a ribbon-type synaptic terminal. *J Neurosci* 17: 1919–1927, 1997.

von Gersdorff H, Sakaba T, Berglund K, and Tachibana M. Submillisecond kinetics of glutamate release from a sensory synapse. *Neuron* 21: 1177–1188, 1998.

von Gersdorff H, Schneggenburger R, Weis S, and Neher E. Presynaptic depression at a calyx synapse: the small contribution of metabotropic glutamate receptors. *J Neurosci* 17: 8137–8146, 1997.

von Gersdorff H, Vardi E, Matthews G, and Sterling P. Evidence that vesicles on the synaptic ribbon of retinal bipolar neurons can be rapidly released. *Neuron* 16: 1221–1227, 1996.

Wang LY and Kaczmarek LK. High-frequency firing helps replenish the readily releasable pool of synaptic vesicles. *Nature* 394: 384–388, 1998.

Wu LG and Borst JG. The reduced release probability of releasable vesicles during recovery from short-term synaptic depression. *Neuron* 23: 821–832, 1999.

Zeger SL and Liang KY. Longitudinal data analysis for discrete and continuous outcomes. *Biometrics* 42: 121–130, 1986.

Zidanic M and Fuchs PA. Kinetic analysis of barium currents in chick cochlear hair cells. *Biophys J* 68: 1323–1336, 1995.

Zucker RS. Short-term synaptic plasticity. *Annu Rev Neurosci* 12: 13–31, 1989.